Chitosan Nanoparticles for Loading of Toothpaste Actives and Adhesion on Tooth Analogs

Hui Liu, Bo Chen, Zhengwei Mao, Changyou Gao

Key Laboratory of Macromolecule Synthesis and Functionalization, Ministry of Education, Department of Polymer Science and Engineering, Zhejiang University, Hangzhou 310027, China

Received 28 April 2007; accepted 28 June 2007
DOI 10.1002/app.27078
Published online 7 September 2007 in Wiley InterScience (www.interscience.wiley.com).

ABSTRACT: Delivery and sustained release of toothpaste actives is an important but unexplored area. In this work, chitosan nanoparticles were prepared by a water-in-oil emulsion/glutaraldehyde crosslinking method. The typical number average diameter of chitosan and toothpaste active (cetylpyridiniumchloride and NaF) nanoparticles was within the range of 100–500 nm. The particles increased their size at higher pH value. The morphology, adherence, and stability of these nanoparticles were investigated by scanning electron microscopy, transmission electron microscopy, and X-ray photoelectron spectroscopy. The size of the chitosan/NaF nanoparticles was doubled after they were stored at 4°C for 20 days, and then kept constant till 251 days, the examined time so far. These particles showed good stability in toothpaste lixivium after incubated at 60°C for 30 days too. By contrast, the chitosan/cetylpyridiniumchloride nanoparticles were easy to form floccules in the toothpaste lixivium. The loaded toothpaste actives showed a sustained released behavior for at least 10 h. All the particles could adhere onto the tooth analogs such as hydroxyapatite discs and glass slides in a simulated brushing and rinsing process. *In vitro* cell culture did not find any cytotoxicity of the as-prepared chitosan nanoparticles. © 2007 Wiley Periodicals, Inc. J Appl Polym Sci 106: 4248–4256, 2007

Key words: adhesion; chitosan nanoparticles; emulsion crosslinking; toothpaste actives

INTRODUCTION

Decayed tooth is one of the oral diseases badly influencing the daily life of people. The tooth walls are frequently and unavoidably corroded by a great amount of acidic substances which are produced by remnant food, making the teeth fragile and leading to the tooth erosion finally. The tooth surface is mainly composed of hydroxyapatite (HA), which has equilibrium in saliva as shown in Eq. (1):

$$Ca_5(PO_4)_3OH \underset{\text{mineralization}}{\overset{\text{demineralization}}{\rightleftharpoons}} 5Ca^{2+} + 3PO_4^{3-} + OH^- \quad (1)$$

Besides of teeth brushing to remove the remnant foods, toothpaste actives such as fluorine ions can harden the teeth by forming a more stable compound, which has stronger ability against acid erosion, as shown in Eq. (2):

$$5Ca^{2+} + 3PO_4^{3-} + F^- = Ca_5(PO_4)_3F \downarrow \quad (2)$$

Thus, the fluorine ions are beneficial of tooth remineralization, reducing the occurrence of dental caries.[1] On the other hand, cetylpyridiniumchloride (CPC, $C_{21}H_{38}ClN{\cdot}H_2O$) is another multifunctional antibacterial drug with good attachment ability on skin, which is suitable for persisting antibacterial application. However, a simple addition of these toothpaste actives has a very short-term effect on the teeth, i.e. during the course of teeth brushing. After gargling, the actives are mostly lost. Drug delivery system is an effective way to realize the sustained release of many kinds of drugs, yet it is scarcely applied to the toothpaste actives.

Chitosan has been applied widely in the medical pharmaceutical fields.[2] It has abundant amino and hydroxyl groups in its molecule, thus can bind strongly to negatively charged substances such as cell surfaces, mucus or other polymer surfaces via electrostatic or hydrogen bonding. Therefore, chitosan is extremely useful as vehicle for mucoadhesion drug delivery.[3] Moreover, chitosan also can accelerate the wound healing, inhibit bacteria growth, and alleviate pain.[4,5] Since the tooth surface is electronegative, we expect that the positively charged chitosan

Correspondence to: C. Y. Gao (cygao@mail.hz.zj.cn).
Contract grant sponsor: Major State Basic Research Program of China; contract grant number: 2005CB623902.
Contract grant sponsor: Natural Science Foundation of China; contract grant number: 20434030.
Contract grant sponsor: National Science Fund; contract grant number: 50425311.

is one of the best candidate materials as delivery vehicle for toothpaste actives.

Nowadays, chitosan and their derivative materials, in particular with a format of particles, have been diversely employed in the field of drug delivery. Various methods such as emulsion crosslinking,[6,7] ionotropic gelation,[8–10] emulsification/solvent evaporation,[11] spray drying,[12] and coacervation/precipitation[13,14] have been developed to prepare the chitosan microparticles. For example, Thanoo et al. prepared chitosan microspheres (425–600 μm) by glutaraldehyde crosslinking of an aqueous acetic acid dispersion of chitosan in paraffin oil.[6] The highly crosslinked microspheres showed a slower release rate whereas the less crosslinked ones showed a faster rate observed in simulated gastric and intestinal fluids. He et al. prepared both uncrosslinked and crosslinked chitosan microparticles (2–10 μm) by a spray drying method for H_2-receptor antagonists.[12] The positively charged microspheres are beneficial of enhancing the mucoadhesion, enabling them suitable for delivery of drugs via the gastrointestinal or nasal routes of delivery. The mucoadhesive properties of the microspheres can be mediated by the preparation parameters. For example, at a lower crosslinking degree, both the particle size and the mucoadhesive properties were improved. Chitosan microparticles (20–30 μm) have also been prepared by a water-in-vegetable oil emulsion coalescence technique, using metal ions as the chelating reagents.[15]

Because of the special smooth characteristic of tooth surface, the microparticles show very poor adhesion property. More recently, nanoparticles have brought much attention in virtue of their large drug loading capacity, good adsorption performance, and long shelf life. Several techniques have been developed to prepare chitosan nanoparticles. On the basis of the ionic gelation of chitosan with tripolyphosphate anions, the chitosan nanoparticles and copper-loaded nanoparticles were prepared.[16] Antibacterial studies showed that the nanoparticles could inhibit the growth of various bacteria, most probably following a mechanism of membrane disruption and leakage of the cellular proteins. Ultrafine chitosan nanoparticles were also prepared in an AOT (sodium bis(ethylhexyl) sulfosuccinate)/*n*-hexane reverse micellar system and crosslinked by glutaraldehyde.[17] After intravenous injection the nanoparticles could circulate in blood and distribute in the bone marrow.

Up to present, however, the chitosan nanoparticles are scarcely applied as delivery vehicle for toothpaste actives. Besides the physical adsorption of the chitosan molecules on the tooth surface, the very small size of the chitosan nanoparticles benefits the adhesion too. Therefore, in this study, we make use of the chitosan nanoparticles as the delivery vehicle for the toothpaste actives, exemplified here with NaF and CPC. Different from the reported methods for the chitosan nanoparticle fabrication, we adopt here a water-in-oil emulsion dispersion technique, which produces more stable chitosan nanoparticles against agglomeration. The adhesion, drug loading, and release of the chitosan nanoparticles shall also be presented.

MATERIALS AND METHODS

Materials

Chitosan (M_n = 620 kDa, degree of deacetylation = 90%, viscosity = 115 cps) was a commercial product of Haidebei Halobios. (Ji'nan, China). Cetylpyridiniumchloride (CPC), NaF, and Crest toothpaste (containing NaF and SiO_2 particles besides toothpaste basic components) were kindly provided by P&G. (Guangzhou, China). Glutaraldehyde (25% solution) and lysozyme were of biological grade. HA discs were from Hitemco Medical Application, USA. Bovine serum albumin (BSA) and fetal calf serum (FCS) were purchased from Sijiqing Biotech (Hangzhou, China). Dulbecco's minimum essential medium (DMEM) was purchased from GibcoBRL. All other chemicals were of analytical grade and used as received. The water used in all experiments was triple distilled.

Preparation of the chitosan nanoparticles

The chitosan nanoparticles, either loaded with drugs or not, were prepared by an emulsion dispersion technique. In a typical experiment, in a 250 mL round-bottom flask 100 mL olive oil was mixed with 1 mL Span 80 and 0.25 g magnesium stearate at room temperature. Four milliliter of 1% chitosan solution in 3 vol % acetic acid was diluted to 20 mL with water (final concentration 2 mg/mL), which was then poured into a flask. The mixture was stirred at 450 rpm for 1 h with a mechanical stirrer to form a water-in-oil emulsion. 0.5 mL of 3.1% glutaraldehyde solution was injected into the mixture to crosslink the chitosan molecules and stabilize the chitosan nanoparticles. Two hours later, the temperature was improved to 40°C by a water bath. Under agitation at 400 rpm the reaction was continued for 6 h. After the oil layer was separated, the pH value of the water phase was adjusted to ~8 by 0.1*M* NaOH under vigorous agitation. The water phase was then centrifugated at 3000 rpm to remove the unreacted chitosan and bigger particles. Finally, the supernatant was adjusted to neutral pH and stored at 4°C. The drug-loaded nanoparticles were similarly prepared by using a chitosan solution containing the drugs.

Morphology of the chitosan nanoparticles

Scanning electron microscopy (SEM; SIRION-100, FEI), transmission electron microscopy (TEM; JEOL JEM-200CX, Japan), and scanning force microscopy (SFM; SPI3800N Probe Station and SPA400 SPM Unit, Seiko) were used to observe the chitosan nanoparticles. The samples were prepared as follows.

SEM: A drop of the nanoparticle suspension was applied onto a HA disc or a H_2O_2/H_2SO_4 (3/7, v/v) treated (1 h) glass slide, dried at 40°C and fixed on an aluminum stub with a conductive adhesive tape, then sprayed with a gold layer under vacuum with a Sputter Coater Edwards S 150A. The nanoparticles were observed also after freeze-dried. The acceleration voltage was 5 kV.

TEM: A drop of the nanoparticle suspension was applied onto a carbon-coated copper meshwork, dried at room temperature. The acceleration voltage was 100 kV.

SFM: A drop of the particle suspension was applied onto newly cleaved mica, dried at 40°C. Silicon tips with a resonance frequency f_0 of 150 kHz and a spring constant of 16 N/m were utilized. The scanning frequency was 1 Hz.

Size of the chitosan nanoparticles

The size of the nanoparticles was measured by a dynamic light scattering particle size analyzer (DLS) (90 Plus/BI-MAS). Each measurement was taken for 1 min with a 90° fixed angle detector. The diameter was averaged from five parallel measurements.

Loading amount of the toothpaste actives

The nanoparticles containing the drugs were centrifugated at 8000 rpm for 10 min to obtain the nanoparticle precipitate, which was washed with water twice, and freeze-dried. 5.1 mg freeze-dried chitosan/CPC nanoparticles were then dispersed in 10 mL ethanol under continuous shaking for 12 h to dissolve the CPC. After centrifugation, the absorbance of the supernatant at 259 nm was recorded by a UV–vis spectrophotometer (Shimadzu UV-2550). The concentration was quantified by referring to a calibration curve recorded from known amount of CPC at the same condition.

For determination of the NaF amount, the chitosan/NaF nanoparticle precipitate was dispersed in 3 mL lysozyme solution (10 mg/mL) at 37°C for 5 days to degrade the chitosan molecules completely. After centrifugation, the supernatant was collected and the potential of fluorine was measured by a fluorine ion-selective electrode, with 10 mL citrate sodium as whole regulating regent of ion intensity, 7.5 mL water and certain amount of PBS to maintain 20 mL finally. The concentration was quantified by referring to a calibration curve recorded from known amount of NaF at the same condition.

The loading capacity was calculated by the drug weight/the particle weight × 100%.

Release of the toothpaste actives

The CPC release was performed by putting 20.2 mg nanoparticles into a dialytic-bag (cut-off molecular weight Mw: 8–14.4 kDa). The bag was then immersed into 30 mL PBS (pH 6.8) at 37°C under continuous shaking. The dialytic PBS was exchanged every 1 h. The release of NaF was performed by dispersing 4 mg freeze-dried nanoparticles in 3 mL PBS (pH 6.8) at 37°C under continuous shaking. The nanoparticle suspension was periodically centrifuged and 1.5 mL supernatant was exchanged with the same volume of freshly prepared PBS every 2 h. The released amount of CPC or NaF in the supernatant was quantified as aforementioned.

Adhesion property of the chitosan nanoparticles mixed in toothpaste

The adhesion property of the chitosan nanoparticles was performed by mixing the particles with toothpaste, and under a condition simulating the tooth brushing process. The chitosan nanoparticle suspension was mixed with toothpaste for 1 h. The HA disc or glass slide was immersed in simulated saliva (BSA/PBS 1/4 (v/v), pH = 6.8) for 40 min, then brushed with the chitosan nanoparticle/toothpaste mixture. Finally, the HA disc or glass slide was rinsed with water for 3 times to remove the non-tightly adhered components. After dried, the HA or glass surface was observed under SEM. To detect the adhesion more sensitively and precisely, $CdCl_2$ was incorporated into the chitosan nanoparticles. Following the same mixing and brushing process, the surface elements of the HA disc were determined by X-ray photoelectron spectroscopy (XPS) on an ESCA LAB Mark II spectrometer employing mono X-ray Al Kα ($h\nu$ = 1486.6 eV), 150 w, 15 kV excitation radiation. The base pressure was 2×10^{-9} mbar. The charging shift was referred to the C(1S) line emitted from the saturated hydrocarbon. The take off angle of the XPS was 90°. The constant angle energy was 20 eV.

Stability of the chitosan nanoparticles in toothpaste lixivium

Toothpaste was mixed with certain amount of water, which was centrifugated to get the lixivium. For a speeding up experiment, the nanoparticle suspension/lixivium mixture was kept at 60°C for 30 days.

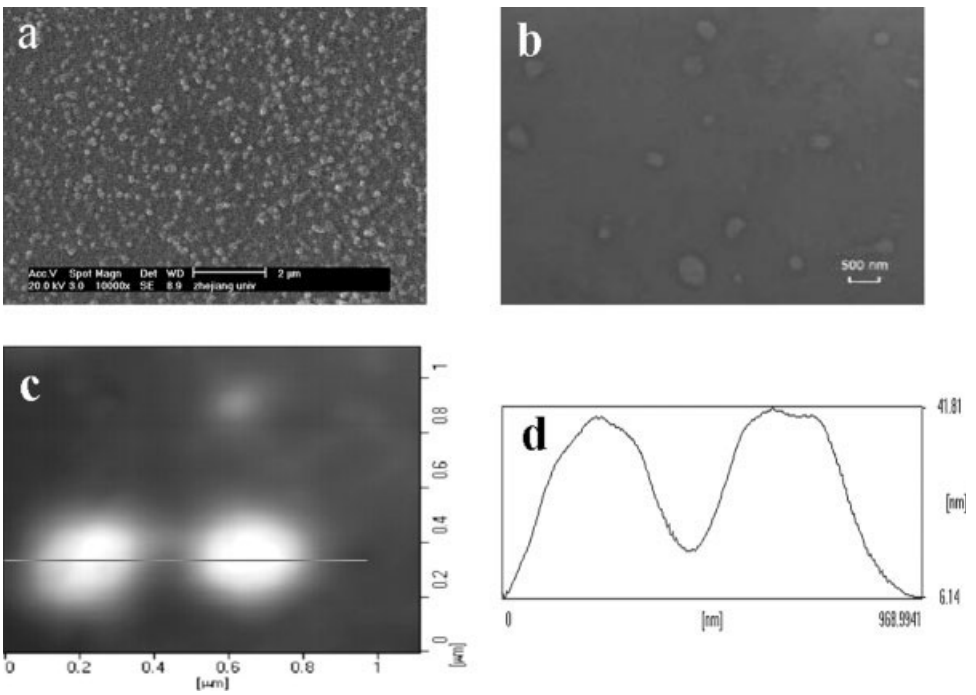

Figure 1 (a) SEM, (b) TEM, and (c) SFM images of chitosan nanoparticles. (d) Line profile recorded at the place shown in (c).

The morphology of the final products was observed under SEM.

Biocompatibility of the chitosan nanoparticles

In vitro cell culture was used to determine the biocompatibility of the as prepared chitosan nanoparticles. Pure chitosan nanoparticles were sterilized by UV irritation before cell culture. Human dermal fibroblasts were isolated from foreskins and routinely expanded.[18] The fibroblasts were incubated in a culture medium consisting of 10% (v/v) FCS and 90% (v/v) DMEM, supplemented with 100 U/mL of penicillin and 100 çg/mL of streptomycin in humidified air containing 5% CO_2 at 37°C. About 200 μL human dermal fibroblast suspension was seeded in a 96-well polystyrene plate, with a final cell number of 7.5×10^4 per well. After 24 h, 20 μL nanoparticle solution was added into each well. The final nanoparticle concentration was high enough for close contact between the cells and the nanoparticles. The culture medium was changed every 2 days. The cell proliferation was measured using methylthiazoletetrazolium (MTT) method.[19] The absorbance was recorded at a wavelength of 570 nm by a microplate reader (Bio-Rad model 550). Three parallel experiments were conducted and data were expressed as mean ± standard deviation.

To observe the cell morphology under SEM, the cells were washed with PBS and fixed with 2.5% glutaraldehyde in PBS at 4°C for 48 h after cocultured with the nanoparticles for 48 h. After washed with PBS to remove the remaining glutaraldehyde, the samples were dehydrated with a graded series of ethanol. Then the samples were further dehydrated with acetone and treated with isoamyl acetate. After dried by the critical point dry method, the samples were coated with ultrathin gold layers and observed under SEM (Cambridge stereoscan 260).

RESULTS AND DISCUSSION

Morphology of the chitosan nanoparticles

Because of the highly sticky property of chitosan molecules, the chitosan particles, in particular in a nanometer range, are rather easy to combine with each other. For example, the as-prepared chitosan nanoparticles without the presence of magnesium stearate formed larger particle clusters. By contrast, addition of the magnesium stearate can largely alleviate the agglomeration of the particles,[20] resulting in well dispersed chitosan nanoparticles [Fig. 1(a)]. The nanoparticles show more condense structure with smoother surface morphology too. Here the nonionic emulsifier, i.e. Span 80, also takes an important role for the particle dispersion during the fabrication process. On the water/oil interface, the nonpolar groups of span-80 and the lipophilic group (stearyl) of magnesium stearate dip into the oil phase, while the three hydroxyls of span-80 and $—COO^-$ of magnesium stearate insert into the aque-

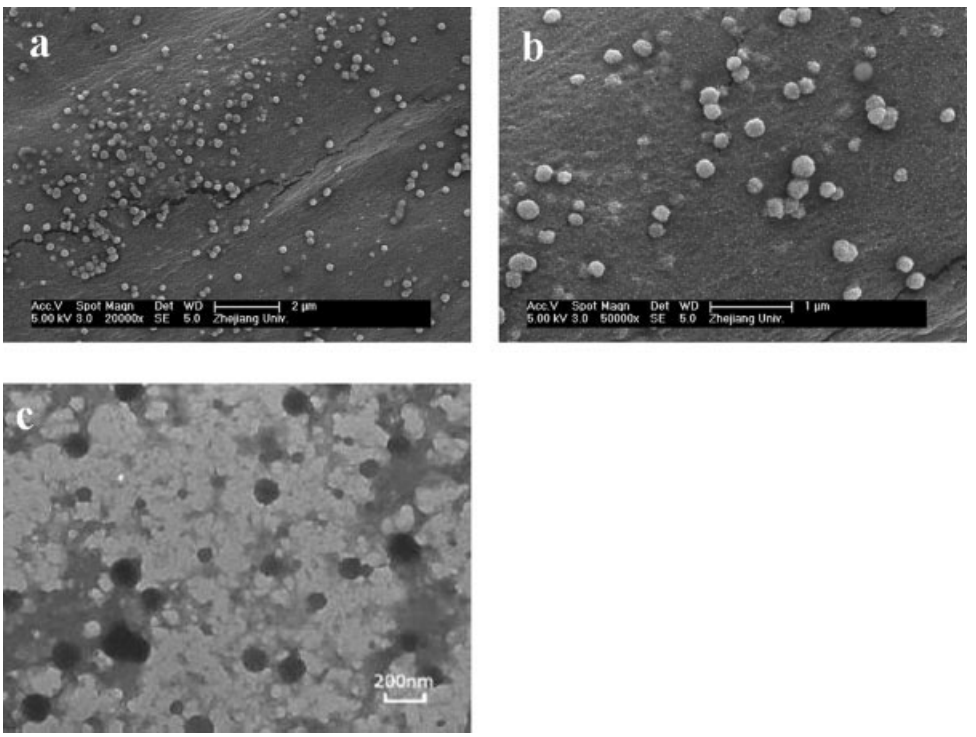

Figure 2 (a) SEM and (c) TEM images of chitosan/NaF nanoparticles. (b) is higher magnification of (a).

ous phase, stabilizing the droplets. Meanwhile, the charged interface can also stabilize the droplets because of the repulsion of the same charge.[21] After crosslinking by glutaraldehyde, the shape and size of the chitosan droplets are fixed. Therefore, by this process the chitosan nanoparticles with good dispersivity are successfully obtained. In the following experiments, all the chitosan particles were fabricated under the existence of magnesium stearate.

The chitosan nanoparticles were further subjected to TEM and SFM characterizations [Fig. 1(b,c)]. Again spherical and well dispersed chitosan nanoparticles can be observed, whose size is consistent with the SEM observation (100–500 nm). No severe agglomeration of the particles was found. The line profile in Figure 1(d) shows that the particles in dry state were collapsed severely, leading to smaller value in height ($\sim$ 40 nm) than that in width. This phenomenon is very common for many ''soft'' polymeric particles, conveying a hint that the chitosan nanoparticles should have a rather loose inner structure. This is reasonable since the theoretical volume in the particles reaches >99% if no condensation occurs during the particle preparation.

The drugs loaded chitosan nanoparticles can be similarly prepared, as shown in Figure 2. Here SEM [Fig. 2(a,b)] and TEM [Fig. 2(c)] images of freeze-dried chitosan/NaF nanoparticles are present as a typical example. Most of the chitosan/NaF nanoparticles are separated from each other, with a size of 100–200 nm. Normally, chitosan nanoparticles with this size tend to aggregate, leading to formation of larger aggregates because of strong interparticle interaction. However, as shown in Figures 1 and 2, the chitosan nanoparticles prepared by the present process have rather good dispersivity, which is crucial for delivery of drug by a mucoadhesive manner.

Size variation of the chitosan/toothpaste active nanoparticles

Measured by DLS, all the chitosan nanoparticles present double peak distribution regardless of the existence of drugs. For example, at pH 8 DLS measured two peaks centered at 140 and 484 nm, while the sizes increased slightly after toothpaste active loading. Because of this nature, in the next discussion, we shall use only the number average diameter to represent the whole samples.

Since the charge density of the chitosan molecules is highly influenced by environmental pH, the particle size may also be varied accordingly. In the present case, when the pH value was increased from pH 7.1–8.3, the average diameter was sharply increased from 29 to 237 nm. This phenomenon is understood as a result of particle coagulation because at high pH the charge degree of the chitosan molecules is reduced. The diminishing charge repulsion between particles will then result in particle aggregation to decrease the surface free energy. Detail study of the

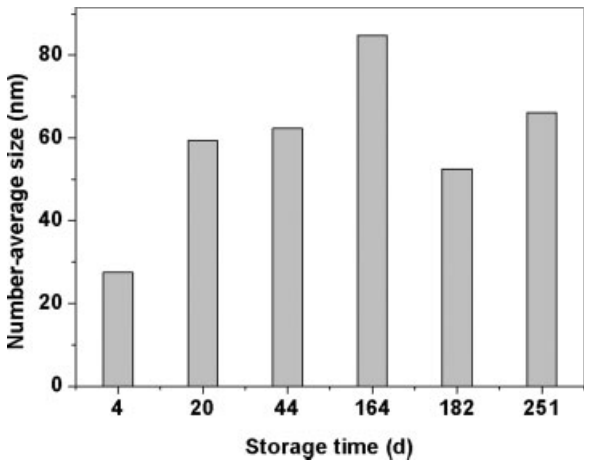

Figure 3 Alteration of average size of chitosan/NaF nanoparticles along with the storage time at 4°C.

pH influence was performed to the chitosan/toothpaste active nanoparticles, since they are the practically applicable delivery systems. Along with the pH increase, both kinds of the nanoparticles increased their sizes with similar alteration tendency. At the same pH value, the size of the chitosan/CPC nanoparticles is always larger than that of the chitosan/NaF nanoparticles. For example, at pH values of 4.5, 7.0, and 8.1, the sizes of the chitosan/CPC nanoparticles were measured as 92, 127, and 194 nm, whereas the sizes of the chitosan/NaF nanoparticles were measured as 4, 46, and 140 nm, respectively. When the pH value was decreased from 8.1 to 7.1, the size of the chitosan/CPC nanoparticles (137 nm) decreased to their initial value again, demonstrating that the aggregation or dispersion of the chitosan nanoparticles is indeed governed by the charge interaction. It has to mention that here the particle aggregation must be taken into consideration, because theoretically the chitosan particles should decrease their size at high pH as a result of reducing intramolecular charge repulsion. This phenomenon has been observed for the ionically crosslinked chitosan particles, in which the particles have smaller size at higher pH.[22] Different crosslinking mechanism may result in different ionic intensity in the particles, leading to the reverse alteration tendency of the particle size in response to pH stimulus.

Furthermore, we observed the sediment in all the chitosan nanoparticle solutions with a pH value higher than 8 after the solutions were stored for a couple of days. This phenomenon reminds us that the chitosan at higher pH value is intrinsically unstable. Because both the toothpaste lixivium and the oral cavity environment are almost neutral, a detail study was performed at pH 7.0 to explore the storage stability, using the chitosan/NaF nanoparticles as a typical example. Here the storage temperature was controlled at 4°C to avoid the environmental temperature fluctuation. Figure 3 shows that the particle size was quickly doubled after 20 days, then reached an equilibrium oscillating between 60 and 80 nm until the examined time so far (251 days). This result demonstrates that the chitosan/NaF nanoparticles are rather stable at neutral pH, at least at low temperature.

Loading and release of toothpaste actives

The loading capacity of CPC and NaF within the chitosan nanoparticles was measured as 14 and 10%, respectively, which are only about 1/4 and 1/5 of the theoretical value. However, these values are not low considering that both drugs are highly water soluble, which may cause the loss during the rinsing steps. The slight higher loading capacity of CPC may result from its relatively larger molecular size, and the existence of long aliphatic hydrocarbon chains.

Both the loaded drugs can be released in a sustainable manner, as shown in Figure 4. An initial burst release was observed for both kinds of nanoparticles, which is a common phenomenon for many drug release systems.[23,24] However, the initial burst release is not severe compared with other systems.[12,25,26] The burst release is known as the result of quick release of the surface adsorbed drugs. Compared with NaF, the CPC was released with a very slow rate. For example, during the first 3 h, 17% of the loaded CPC and 50% of the loaded NaF were released, respectively. These values reached to 33% for CPC and 88% for NaF after 10 h, respectively. The larger molecular size and the hydrophobic hydrocarbon chains should account for the slower release rate of CPC.

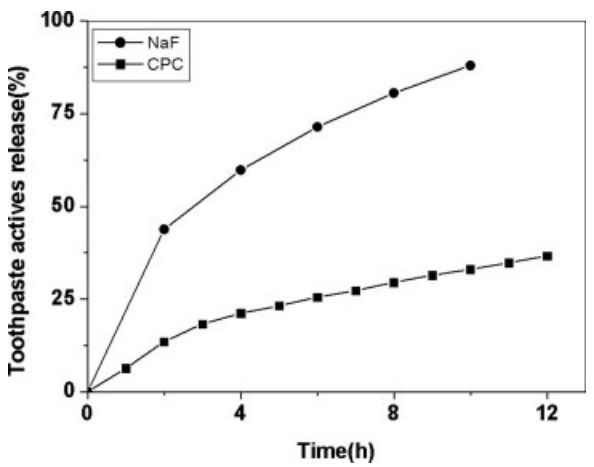

Figure 4 Release profiles of the toothpaste actives from chitosan nanoparticles in PBS (pH 6.8) at 37°C as a function of time.

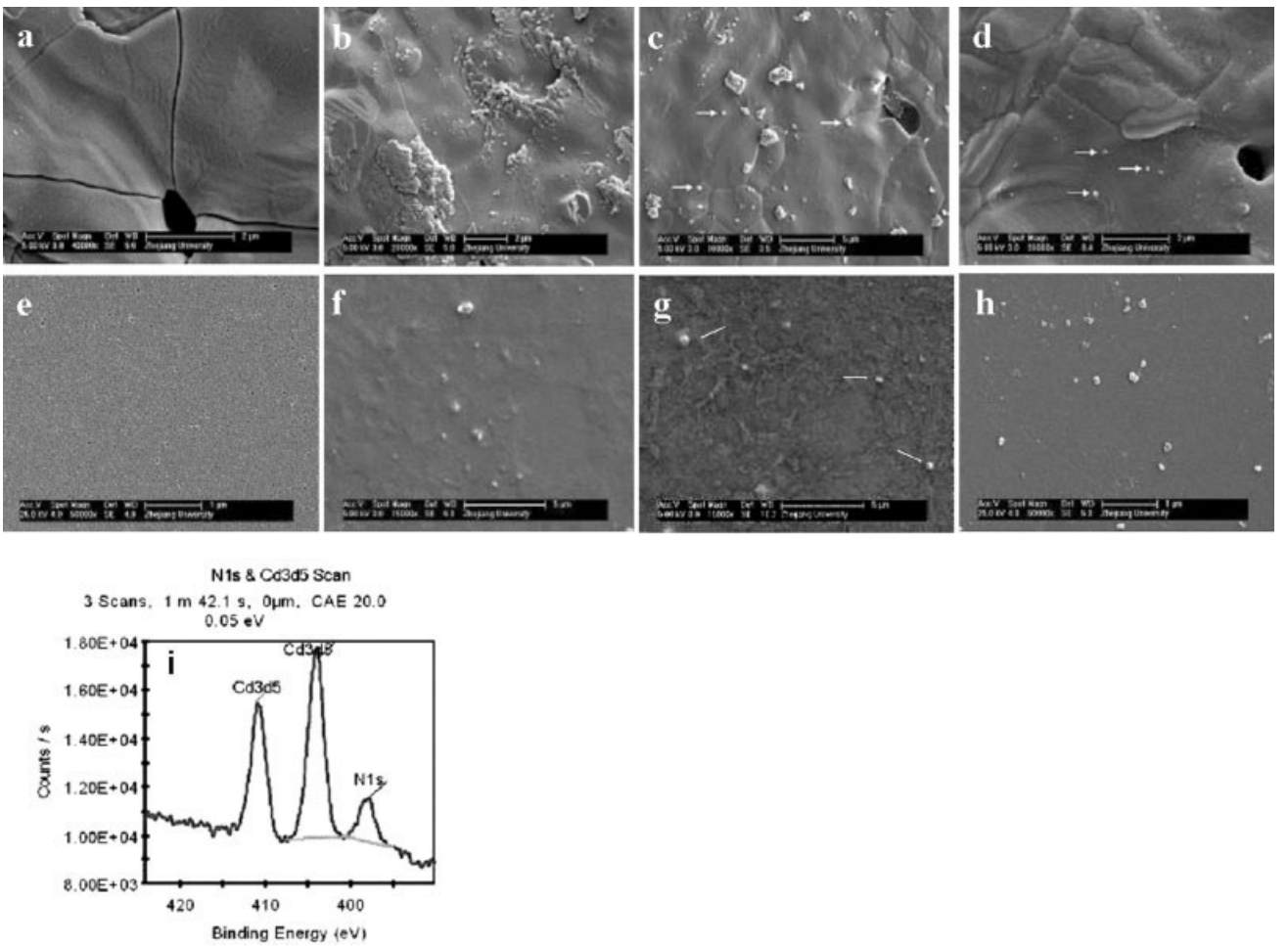

Figure 5 SEM images of chitosan nanoparticles with different actives adhered on HA discs (upper row) or glass slides (lower row). (a,b) HA disc surface, (c) chitosan nanoparticles on HA disc, and (d) chitosan/CPC nanoparticles on HA disc; (e) glass slide surface, (f) chitosan nanoparticles, (g) chitosan/CPC nanoparticles, and (h) chitosan/NaF nanoparticles on the glass slides. Arrows indicate the particles. (i) XPS spectrum to show Cd_{3d5} and N_{1s} scan of HA surface adhered with $CdCl_2$ stained chitosan nanoparticles.

Adhesion property of the chitosan nanoparticles

As a drug delivery vehicle for toothpaste actives, the adhesion property of the drug-loaded particles on the tooth surface is of great importance. *In situ* drug release can be achieved only when the particles are stably adhered. Here we used tooth analogs as the substrates to qualitatively check the adhesion of the chitosan nanoparticles. As shown in Figure 5(a,b), the surface texture of the HA disc is very inhomogeneous, with rough morphology and micron-sized particulates. After brushing the nanoparticle/toothpaste mixture and sufficient rinsing, tiny chitosan and chitosan/CPC nanoparticles can be identified as pointed by the arrows [Fig. 5(c,d)]. To further confirm this adhesion and avoid the interference of the rough surface of the HA disc, planar glass slide was used as a model substrate, since both kinds of materials have plenty of —OH groups and electronegative charge. Compared with the HA disc, the surface of the glass slide is very smooth [Fig. 5(e)]. As shown in Figure 5(f–h), a large number of nanoparticles can be observed on the glass slides, regardless of loading of the drugs.

To unambiguously demonstrate the adhesion of the chitosan nanoparticles on the tooth analogs, the surface chemistry was analyzed by XPS. The survey scan spectrum of the HA disc presents the P, Ca, and O. After brushing with the $CdCl_2$ stained chitosan nanoparticles, extra Cd and N elements can be observed as highlighted in Figure 5(i). Their atomic ratios are between 1.24 and 2.31%, respectively. These results demonstrate the chitosan particles are definitely adhered onto the HA disc surface.

Stability of the chitosan nanoparticles in toothpaste lixivium

The stability in the toothpaste lixivium and adhesion ability after storage in the toothpaste lixivium was

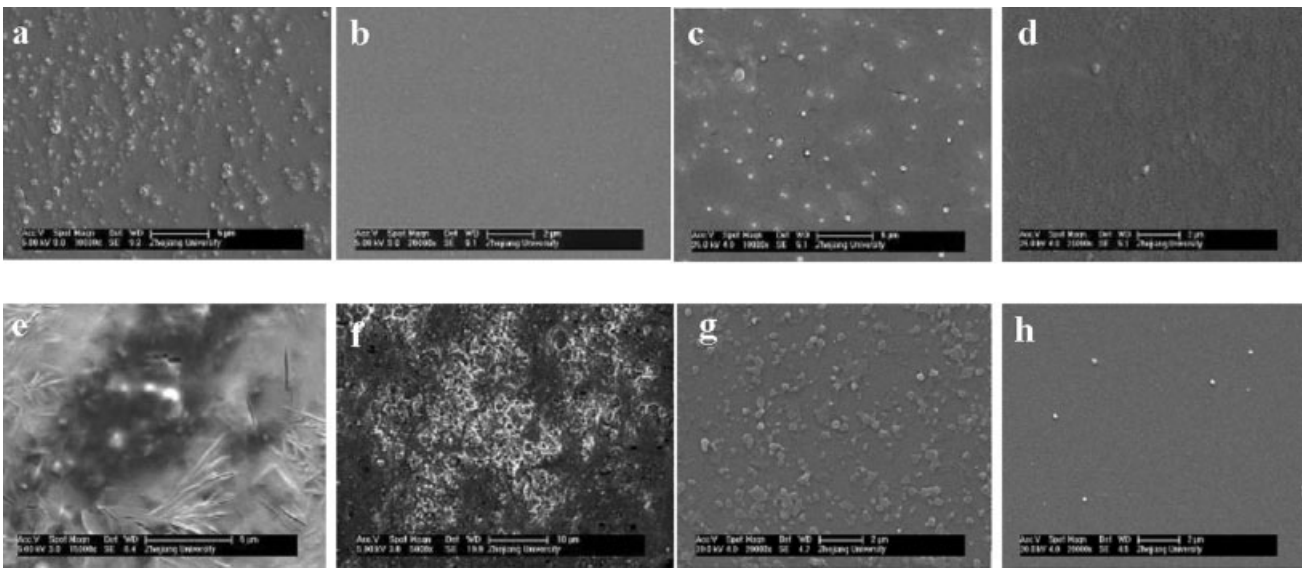

Figure 6 SEM images to show the morphology change. (a) The toothpaste lixivium and (b) its adherence on glass slide; (c) chitosan nanoparticles and (d) their adherence on glass slide after mixed with lixivium and stored at 60°C for 30 days; chitosan/CPC nanoparticles after mixed with the toothpaste lixivium for (e) 10 min and for (f) 30 days (60°C); (g) chitosan/NaF nanoparticles and (h) their adherence after mixed with the toothpaste lixivium and stored at 60°C for 30 days.

qualitatively studied by SEM. As shown in Figure 6(a), submicron particles can be found after the lixivium was dried on glass slide, which may result from the added salt, tiny $CaCO_3$ particles, and other unidentified substances. After rinsing with water, no particulate materials can be found [Fig. 6(b)], indicating that the lixivium itself cannot adhere on the glass slide in a particulate format. When the chitosan particles were suspended in the lixivium at 60°C, no precipitation was observed until 30 days. SEM also shows no floccules in the chitosan particles/lixivium solution [Fig. 6(c)]. After brushing and rinsing, tightly adhered particles can be still found [Fig. 6(d)]. When the chitosan/CPC nanoparticles were mixed with the lixivium, however, floccules were observed within 10 min, as shown in Figure 6(e). The agglomeration became even severe after storage at 60°C for 30 days [Fig. 6(f)]. These results demonstrate that unlike the pure chitosan nanoparticles, the chitosan/CPC nanoparticles in toothpaste lixivium are unstable. CPC is a quaternary ammonium salt having positive charge. It can chelate with saccharides and electronegative surfactants, which are exclusively included in the toothpaste. The chelation will then cause formation of the floccules, and finally precipitation of the chitosan/CPC/lixivium mixture. This was further confirmed by directly mixing CPC and the lixivium, where precipitation occurred immediately. In contrast to the chitosan/CPC nanoparticles, the chitosan/NaF nanoparticles were very stable. No detectable floccules or precipitates were observed macroscopically and microscopically [Fig. 6(g)]. Similar to the chitosan nanoparticles, the chitosan/NaF nanoparticles could adhere on the glass

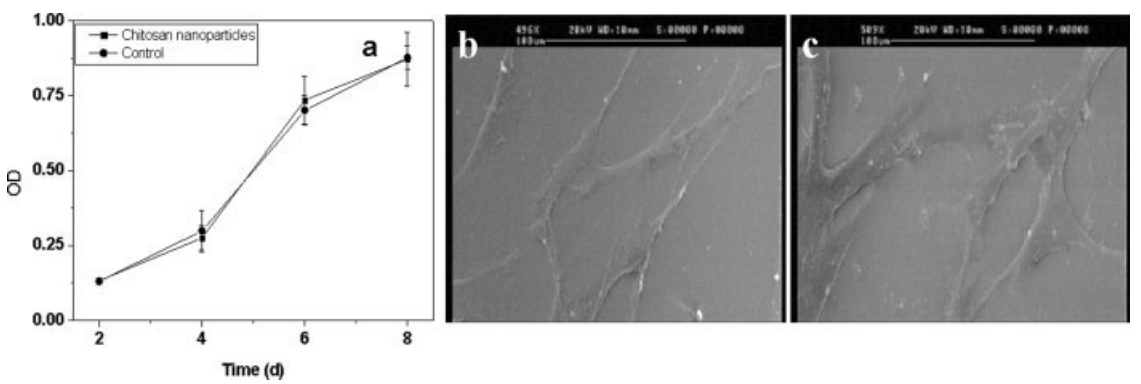

Figure 7 (a) Cytoviability of fibroblasts measured by MTT assay as a function of culture time. Blank control was made by culture medium. And TEM images of fibroblasts cultivated for 24 h without (b) and with (c) the chitosan nanoparticles.

slide firmly too after brushing and rinsing [Fig. 6(h)]. Together with the loading and release property, one can conclude that the chitosan/NaF nanoparticle delivery system possesses a good potential for application in toothpaste.

Biocompatibility of the chitosan nanoparticles

Since the nanoparticles can be uptaken by cells upon contact, it is necessary to assess the influence of the chitosan nanoparticles on the cytoviability. Here only the chitosan nanoparticles were assessed, since the delivery vehicle is the main concern, while the actives themselves have been well studied. For this purpose, *in vitro* culture of human fibroblasts in the presence of the chitosan nanoparticles was performed. Figure 7(a) shows that no significant difference of the cytoviability between the control (cells only) and the samples supplemented with the nanoparticles through all the culture period. The cells in both cases show typical and normal S-shaped growth behavior. Observed under SEM [Fig. 7(b,c)], all the cells show elongated shape, which is typical for the fibroblasts. These results demonstrate that the crosslinked chitosan nanoparticles have not brought detectable cytotoxicity, hence can be safely used as the delivery vehicle for the toothpaste actives.

CONCLUSIONS

Chitosan nanoparticles with an average number diameter of 100–500 nm, either loaded with toothpaste actives or not, were prepared by a water-in-oil emulsion technique, following by GA crosslinking. SEM, TEM, and SFM characterizations revealed that the chitosan molecules and the loaded drugs were evenly distributed within the particles, instead of forming a core-shell structure. The chitosan nanoparticles showed good stability at neutral pH, while precipitate quickly at alkaline condition with increased particle size at the initial stage. The loaded drugs could be sustained released at least for 10 h, with a release percentage of 33% for CPC and 88% for NaF, respectively. The nanoparticles can adhere onto tooth analogs such as HA discs and glass slides, which are confirmed by direct SEM observation and XPS analysis. Floccules were formed when the chitosan/CPC nanoparticles were mixed with toothpaste lixivium. By contrast, the chitosan/NaF nanoparticles showed very good stability with respect to long term storage in both pure water and toothpaste lixivium. Therefore, one can predict that the chitosan nanoparticles have great potentials to be used for delivery of toothpaste actives and for *in situ* release of the actives in a sustained manner.

References

1. Wang, B. B.; Zheng, B. S.; Zhai, C.; Yu, G. Q.; Liu, X. J. Environ Int 2004, 30, 1067.
2. Illum, L. Pharm Res 1998, 15, 1326.
3. Sinha, V. R.; Singla, A. K.; Wadhawan, S.; Kaushik, R.; Kumria, R.; Bansal, K.; Dhawan, S. Int J Pharm 2004, 274, 1.
4. Howling, G. I.; Dettmar, P. W.; Goddard, P. A.; Hampson, F. C.; Dornish, M.; Wood, E. J. Biomaterials 2001, 22, 2959.
5. Okamoto, Y.; Kawakami, K.; Miyatake, K.; Morimoto, M.; Shigemasa, Y.; Minami, S. Carbohydr Polym 2002, 49, 249.
6. Thanoo, B. C.; Sunny, M. C.; Jayakrishnan, A. J Pharm Pharmacol 1992, 44, 283.
7. Genta, I.; Costantini, M.; Asti, A.; Conti, B.; Montanari, L. Carbohydr Polym 1998, 36, 81.
8. Pan, Y.; Li, Y. J.; Zhao, H. Y.; Zheng, J. M.; Xu, H.; Wei, G.; Hao, J. S.; Cui, F. D. Int J Pharm 2002, 249, 139.
9. Berger, J.; Reist, M.; Mayer, J. M.; Felt, O.; Peppas, N. A.; Gurny, R. Eur J Pharm Biopharm 2004, 57, 19.
10. Ko, J. A.; Park, H. J.; Hwang, S. J.; Park, J. B.; Lee, J. S. Int J Pharm 2002, 249, 165.
11. Genta, I.; Perugini, P.; Conti, B.; Pavanetto, F. Int J Pharm 1997, 152, 237.
12. He, P.; Davis, S. S.; Illum, L. Int J Pharm 1999, 187, 53.
13. Bayomi, M. A.; Al-Suwayeh, S. A.; El-Helw, A. M.; Mesnad, A. F. Pharm Acta Helv 1998, 73, 187.
14. Vandenberg, G. W.; Drolet, C.; Scott, S. L.; De La Noue, J. J Control Release 2001, 77, 297.
15. Kofuji, K.; Qian, C. J.; Murata, Y.; Kawashima, S. React Funct Polym 2005, 62, 77.
16. Qi, L. F.; Xu, Z. R.; Jiang, X.; Hu, C. H.; Zou, X. F. Carbohydr Res 2004, 339, 2693.
17. Banerjee, T.; Mitra, S.; Singh, A. K.; Sharma, R. K.; Maitra, A. Int J Pharm 2002, 243, 93.
18. Mao, Z. W.; Ma, L.; Gao, C. Y.; Shen, J. C. J Control Release 2005, 104, 193.
19. Liu, Y. Y.; Yoshikoshi, A.; Wang, B. C.; Sakanishi, A. Colloid Surf B Biointerfaces 2003, 27, 287.
20. Bogataj, M.; Mrhar, A.; Grabnar, I.; Rajtman, Z.; Bukovec, P.; Srcic, S.; Urleb, U. J Microencapsul 2000, 17, 499.
21. Lim, L. Y.; Wan, L. S. C. J Microencapsul 1998, 15, 319.
22. López-León, T.; Carvalho, E. L. S.; Seijo, B.; Ortega-Vinuesa, J. L.; Bastos-González, D. J Colloid Interface Sci 2005, 283, 344.
23. Ozbas-Turan, S.; Akbuga, J.; Aral, C. J Pharm Sci 2002, 91, 1245.
24. Janes, K. A.; Fresneau, M. P.; Marazuela, A.; Fabra, A.; Alonsoa, M. J. J Control Release 2001, 73, 255.
25. Zhou, S. B.; Deng, X. M.; Li, X. H. J Control Release 2001, 75, 27.
26. Wu, Y.; Yang, W. L.; Wang, C. C.; Hu, J. H.; Fu, S. K. Int J Pharm 2005, 295, 235.